A Coherent Algorithm for Noise Revocation of Multispectral Images by Fast HD-NLM and its Method Noise Abatement

Vijayalaxmi Hegde11† , Basavaraj N. Jagadale2††, and Mukund N. Naragund3†††

Kuvempu University, Jnanasahyadri, Shankaraghatta, India

Abstract

Numerous spatial and transform-domain-based conventional denoising algorithms struggle to keep critical and minute structural features of the image, especially at high noise levels. Although neural network approaches are effective, they are not always reliable since they demand a large quantity of training data, are computationally complicated, and take a long time to construct the model. A new framework of enhanced hybrid filtering is developed for denoising color images tainted by additive white Gaussian Noise with the goal of reducing algorithmic complexity and improving performance.

In the first stage of the proposed approach, the noisy image is refined using a high-dimensional non-local means filter based on Principal Component Analysis, followed by the extraction of the method noise. The wavelet transform and SURE Shrink techniques are used to further culture this method noise. The final denoised image is created by combining the results of these two steps.

Experiments were carried out on a set of standard color images corrupted by Gaussian noise with multiple standard deviations. Comparative analysis of empirical outcome indicates that the proposed method outperforms leading-edge denoising strategies in terms of consistency and performance while maintaining the visual quality.

This algorithm ensures homogeneous noise reduction, which is almost independent of noise variations. The power of both the spatial and transform domains is harnessed in this multi realm consolidation technique. Rather than processing individual colors, it works directly on the multispectral image. Uses minimal resources and produces superior quality output in the optimal execution time.

Key words:

AWGN; PSNR; SSIM; Wavelet Thresholding; NL-Means Algorithm.

1. Introduction

Images will unavoidably be distorted with varying degrees of random noise during the process of acquisition (due to limitations of the optics or inadequate illumination [1]), transmission (due to channel problems), and storage. In presence of noise, the quality and appearance of the image will get deteriorated and further analysis of the image such as segmentation, tracking, video processing, and feature extraction becomes strenuous [2]. Hence, denoising is one of the indispensable and prefatory paces in image processing.

Buades et al [3] propose three norms of denoising an image. The first criterion expects that noise and just noise must be removed from an image. When we employ any algorithm for denoising an image, the distinction between the original image and its denoised form indicates the "noise" removed by that algorithm. This remnant is called "method noise"[4].

The second rule, noise to noise [3], requires that the denoising algorithm transforms a white noise into white noise. This conflicting specification is by all accounts the ideal approach to portray accurate calculations. It is sensible for a mathematical assessment. Mathematical and experimental contentions show that bilateral and NL-Means filters are the main ones fulfilling the clamor-to-commotion rule.

The third principle, statistical optimality is limited to neighborhood filters [4]. It doubts if a given area channel can recover dependably the neighborhood J(i) of any pixel i. NL-Means filter best suits this essential.

Nowadays, color images are invariably used all over. In the process of denoising of color images, it is indispensable to retain structural fine highlights (edges, lines, and corners) of the image along with color details. In the recent past, abundant methods and algorithms have been developed to denoise the images [5], [6], [7]. Lion's share of these computations can be used especially for grayscale pictures. It is hard to utilize them for color images while saving their efficacy. Real-time implementation of denoising of multispectral and hyper spectral images has consistently been a challenge because of larger range dimensions [8]. Any computation pertinent for grayscale denoising can likewise be applied for the channel-by-channel handling of high dimensional images [8]. However, working with the combined intensity space can bring out an extreme inter-channel correlation [9].

A greater number of high-dimensional denoising algorithms employ non-linear filters such as bilateral [10], [9] joint bilateral [11], and non-local means filters [12].

Manuscript received December 5, 2021
Manuscript revised December 20, 2021
https://doi.org/10.22937/IJCSNS.2021.21.12.77

1.1 Non-Local Means Filter

It is a kind of non-linear neighborhood filter, appropriate for isolating Gaussian noise while safeguarding edges and subtleties of the original images.

The NLM technique was proposed by Buades et al [3].

Under the Gaussian commotion proposition, the weights are determined, which are utilized to gauze the equivalence between a central region patch and its neighborhood patches in the searching window.

Any RGB color image f is generally characterized by an array of [H, W, 3], where each pixel is a three-component vector of integer values in the distance of [0,255]. (K=3, represents three channels).

The non-local method is represented by equations 1 and 2 [13].

$$g_{k(x,y)} = \frac{\sum_{u,v\in N} f_{k\,(x+u,y+v)}\, W(u,v)\,)}{\sum_{u,v\in N} W(u,v)} \quad (1)$$

Where,

$$W(u,v) = \exp - \frac{\sum_{p\in P} \left\| f_k(x+p,y+p) - f_k(x_0+p,y_0+p) \right\|_2^2}{h^2} \quad (2)$$

Where N is the seeking window,

P is the patch window,

h is the boundary to control the degree of flawlessness, gk is the sifting result,

W(u,v) is the weight that utilizes pixel data to quantify the resemblance between the central area patch and its neighborhood patches.

In (Eq.2), ||• ||2 is Euclidian distance.

(x0,y0) is the position of the central pixel.

(x,y) is the position of the neighboring pixel in the seeking window. Each one of the pixels is filtered by (Eq.1).

1.2 Fast Non-Local Means Filter (Fast NLM)

In NLM, "if f(i) is the noisy image contaminated with AWGN and p(i) is the square patch of pixels around i. If the patch is m × m, then the dimension of p(i) is ρ = 3m2 for color images." Speed of NLM is increased and computational intricacy of NLM is lowered by projecting the patch onto a low-dimensional space utilizing principal component analysis (PCA) [14].

Limitations

Experimental results show that spatial filters eliminate noise to a reasonable amount but at the cost of image blurring, which in turn loses sharp edges [2]. Further, non-local methods remove noise better but, structural information is not well preserved by non-local methods, which degrades the visual image quality [2]

1.3 Wavelet Denoising

Proposed by Donoho in 1994 [15], wavelet transform-based denoising is one of the classical transform domain filtering methods of separating desired information from noisy images [16], [3].

The wavelet transform carries out a correlation examination: Accordingly, the productivity is projected to be maximal when the input image matches to a large amount, the mother wavelet.

Suppose an image has, its energy packed in a limited length of wavelet dimensions, its coefficients will be comparably greater than some other signal or clamor that its energy spreads over an enormous number of coefficients. Shrinking the wavelet transform will remove the low amplitude noise in the wavelet domain, the inverse wavelet transform will then recover the required image with a slight loss of information.

Wavelet denoising steps [14]:

Decompose the image using DWT[15].

Choose the wavelet type and the number of decomposition levels.

Perform thresholding by shrinking the coefficients.

Reassemble the image by computing inverse wavelet transform. (IDWT).

Thresholding

Hard and soft thresholding approaches (proposed by Donoho and Johnston [15]) are generally used to get rid of small coefficients in the filtering process. In hard thresholding, the wavelet coefficients less than a certain value are set to zero, while in soft thresholding, the wavelet coefficients are reduced by a specific amount to the threshold level. The threshold value is the measurement of the noise level, which is normally decided by the standard deviation of the detailed coefficients.

Empirical evidence shows that soft thresholding furnishes smoother results in comparison with hard thresholding. One can retrieve visually pleasant images since it is continuous. The hard threshold furnishes better edge conservation than the soft one. Sometimes it is better to apply the soft threshold to few detail levels, and the hard one to the rest.

There are various adaptive thresholding techniques [17], [18]such as VISUShrink, BayeShrink, NeighShrink, SmoothShrink, and NeighLevel [19] which can give better denoising results than hard and soft thresholding. [20], [21], [22].

1.3.1 SURE Shrink

Proposed by Donoho & John Stone [15], is a sub-band adaptive thresholding technique based on Stein's

Unbiased Risk Estimate. It aims to choose thresholds that adust to the data as well as curtail the assessment of Mean Square Error (MSE). It imparts a portent of the accuracy of a given estimator. This is crucial since, in deterministic estimation, the genuine MSE of an estimator generally depends on the value of the unknown parameter, and thus cannot be resolved totally.

SURE Shrink attempts to select threshold TSURE, which adapts to the data in addition to the reduction of estimation of Mean Square Error (MSE). The threshold parameter TSURE is calculated using equation (3).

$$T_{SURE} = \operatorname{argmin}_{T_h}\left(SURE(T_h; W)\right) \tag{3}$$

Where,

$$\begin{aligned} &\left(SURE(T_h; W)\right. \\ &= @\sigma_n^2 \\ &-\frac{1}{L}\, x \left(2\sigma_n^2, \#\left\{i: |W_i|\right.\right. \\ &\left.\left.\leq T_h - \sum_{i=1}^{L} \operatorname{mean}(|W_i|, T_h)^2\right\}\right) \end{aligned} \tag{4}$$

Where, $\sigma_n^2$is the noise variance, L is the total number of wavelet coefficients in a particular subband, W_i is a wavelet coefficient in a particular subband, $T_h \in [0, T_u]$, T_u is the universal threshold.

Limitations of the wavelet transform denoising model

Even though wavelet transform is an effective method to remove the Gaussian noise, it can introduce visual antiquities in the denoised output of natural images because one fixed wavelet basis cannot represent diverse local structural patterns [23].

Investigation and evaluation of preceding denoising algorithms have presumed that utilizing the hybrid technique of spatial filtering and “discrete wavelet transform” can be viewed as a compelling strategy to get the advantage of the two sides and bring out better denoising output while retaining the attributes of the images [24].

2. Related Work

Shreyamsha Kumar [25] proposed the technique of amalgamation of “Non Local Means filter and its method noise thresholding using wavelet transform” for gray scale images.

By approximating both data and the kernel, Pravin Nair and Kunal N Chaudury [8] suggested a structure for high-speed,high dimensional filtering. They devised a formula that combines information’s flexibility with the kernel’s estimated capability. The shiftable approximation model is used. An effective approach for selecting the movements (centers) and coefficients was proposed using K-means segmentation and data driven smoothing. This computation was shown to be emulous with existing color image filtering algorithms for rapid bilateral and non-local means filtering.

The proposed image-filtering model is intended to accomplish the following objectives:

1. Its effectiveness should be comparable in terms of peak signal to noise ratio and image quality.
2. It should provide stabilized denoising performance across a range of noise levels.
3. Compact and should have the lowest computing cost possible.

2.1 Proposed Model

By using the method noise extraction methodology and then thresholding the noisy wavelet coefficients using SURE shrinking strategy, our model attempted to improve the performance of Pravin Nair’s rapid high-dimensional NLM filtering variation[26].

Our proposed algorithm is a two-stage denoising model.

At the primary stage, the colour image debased by AWGN was passed through a PCA-based NLM smoothing version of the rapid high dimensional filter.

The following stage recognised method noise in the first stage's output and filtered it using a "level 2 discrete wavelet transform with sym4 wavelets and SURE thresholding."

The final denoised image is created by combining the results of these two methods.

2.2 Agorithm of The Proposed Model:

1) Color image f contaminated by Additive White Gaussian Noise (AWGN) of given variance.
2) Fast High Dimensional denoising with K-number of clusters and filtering with Principal Component Analysis based Non-Local Means Filter(PCA-NLM). fNLM
3) Method noise extraction. fMN =f – fNLM
4) Application of discrete wavelet transform of level 2 using sym4 wavelets and decomposing fMN into “approximation and detailed” coefficients.
5) Extraction of “detailed coefficients” and thresholding with SURE (Stein Unbiased Risk Estimate) technique.
6) Inverse wavelet transform fDWN.
7) Combine steps 2 and 6 to get the final image. fDEN= fNLM + fDWN.

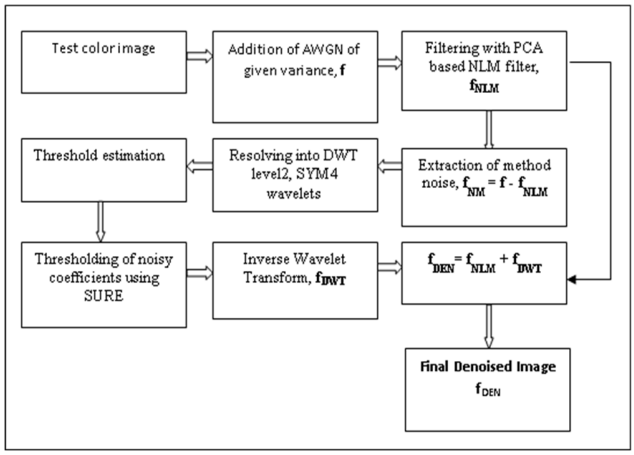

Figure 1. Flowchart of the proposed denoising model.

3. Materials and Methods

Implementation of the proposed model was made using Matlab programming language R2020a. CPU used was Intel core I7-2640M with 4 GB RAM. The experiments pointed towards surveying and investigating the performance of the proposed denoising technique against other existing models. An extensive set of trials have been carried out with different image formats (.jpg, .png, .bmp) of the standard color image dataset available on the internet and Matlab library. Denoising parameters such as PSNR, SSIM, and NMSE are calculated using standard built-in functions of Matlab.

Performance Metrics

3.1 PSNR (Peak Signal to Noise Ratio)

PSNR is the extent between the highest possible signal power and the contaminating noise power that impacts the consistency of its portrayal. The PSNR is often utilized as a measure of quality re-creation of an image. High estimation of PSNR denotes the high caliber of the image. It is described using the Mean Square Error (MSE) and relating bending metric.

$$\mathrm{PSNR} = 20\log_{10}\frac{\mathrm{MAX_i}}{\mathrm{MSE}} \tag{5}$$

Where MAXi is the maximum possible pixel value of the image and MSE is Mean Square Error between the filtered image and the original image.

3.2 Mean Squared Error (MSE)

MSE is evaluated by averaging the squared power of the input and the output image pixels.

$$\mathrm{MSE} = \frac{1}{\mathrm{M.N}}\sum_{i=0}^{M-1}\sum_{j=0}^{N-1}\left[\left(\mathrm{I(i,j)}\right) - \left(\mathrm{K(i,j)}\right)\right]^2 \tag{6}$$

Where K(i, j) and I(i, j) are input and output images respectively, and M and N are the width and the height of the images and, (i, j) are the row and column pixels of both original and the resultant images. When two images become identical, MSE holds the value zero.

3.3 SSIM (Structure Similarity Index Measure)

SSIM is used for estimating the resemblance between two images.

The SSIM index is a measure of the quality of proportion of the test image and the reference image.

The mean structural similarity index (MSSIM) calculation: Initially, original and deformed images are separated into squares of size 8 x 8, and afterward, the chunks are converted to vectors. Now, means, μx and μy, standard derivations, σx, and σy and covariance value σxy are assessed.

The luminance l(x, y), contrast c(x, y), and structure correlation s(x, y) based on factual qualities are also estimated.

$$\mathrm{SSIM(x,y)} = \frac{[2\mu_x\,\mu_y+c_1][2\sigma_{xy}+c_2]}{[\mu_x^2+\mu_y^2+c_1][\sigma_x^2+\sigma_y^2+c_2]} \tag{7}$$

3.4 Mean Absolute Error (MAE)

It is the variation between primary and upgraded image

$$MAE = \left|\left(E(x)\right) - \left(E(y)\right)\right| \tag{8}$$

Where E(x) and E(y) are the average intensities of the original and denoised images respectively.

3.5 Correlation Coefficient(CC)

This parameter is used to measure the interrelationship between two images of the same size.

$$\mathrm{r(x,y)} = \frac{\mathrm{S_{xy}}}{\mathrm{S_x S_y}} \tag{9}$$

The following table depicts the value of r, the correlation coefficient.

Table 1 correlation coefficient values.

r	Meaning
1	Perfect correlation
0	Un correlation
-1	Perfect Anti correlation

4. Results and Discussions

A thorough investigation was carried out on standard test images (Fig.1). namely, eyes_closeup.png, hestain, onion, gantrycrane, Lenacolor.jpg, Peppers.png, hibiscus.bmp, and Tulip.png.

For the image eyes_closeup.png, Table II displays a comparison of the proposed approach with best-in-class algorithms, including neural network based DnCNN. As seen in Table 2, the proposed approach greatly improves PSNR and SSIM. The improvement in image quality can be seen clearly in Fig.3.

Figure 2 : Test images.

Table 2: Performance comparison of different methods.

Comparison results for eyes_closeup.png(640X427),(Ref:Fig-2), sigma=20%			
Method	**PSNR**	**SSIM**	**Time Elapsed**
AM	30.7	0.9	3 sec
DnCNN [27]	36.2	0.93	3.5sec
PND NLM [28]	33.3	0.92	8 min
HDNLM [8]	31.2	0.92	**0.92 sec**
Proposed	**55.0567**	**0.99971**	7.91 sec

Figure 3: Eyes_closeup.png

For Fig.4, 5 and 6, a quantitative assessment of PSNR was performed against various standard methods, inclusive of BM3D and DnCNN. Two distinct noise variations (σ=0.01 and σ=0.03) are chosen in this example. The proposed algorithm wins the competition in both circumstances. The results are shown in table-3.

Figure 4 : Aeroplane image

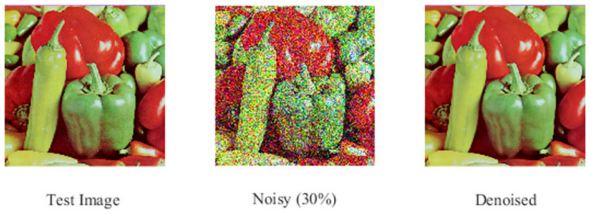

Figure 5 : Peppers image

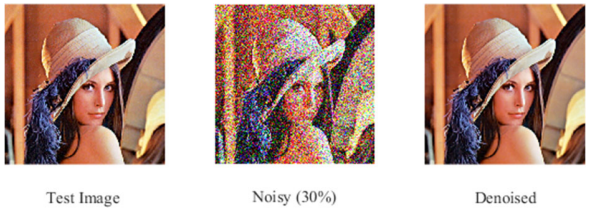

Figure 6: Lena image.

Table 3: Analysis of PSNR for some recent methods

	σ=0.01			σ=0.03		
method	**aeroplane**	**peppers**	**lena**	**aeroplane**	**peppers**	**lena**
Adaptive wavelet	28.0801	27.5706	26.7048	26.4821	25.913	25.4507
Bilateral Filtering	23.1551	23.2116	22.5751	22.6118	22.408	22.0167
Non Local Means[02]	30.1415	29.4155	29.9765	27.6777	27.0736	27.4871
BM3D	30.4215	29.1443	28.9235	27.8901	26.912	26.9276
DnCNN[05]	30.8196	30.373	29.5841	28.1334	28.1737	28.1816
GFAWT[**color]	41.5647	**39.1414**	39.5634	36.0267	34.8926	35.3129
Proposed	**45.2574**	37.3303	**49.2547**	**45.2704**	**37.3958**	**49.5992**

The coherence and consistency of the proposed filtering algorithm are compared to current standards. The proposed standard, as shown in Graph 1 and graph 2, provides consistent and reliable performance for noise levels ranging from 10% to 50%. Other algorithms' performance is inversely proportional to levels, however, the performance of the suggested technique is unaffected by noise levels, as seen in fig. 7, 8, and 9. This is a novel feature, unique to this algorithm.

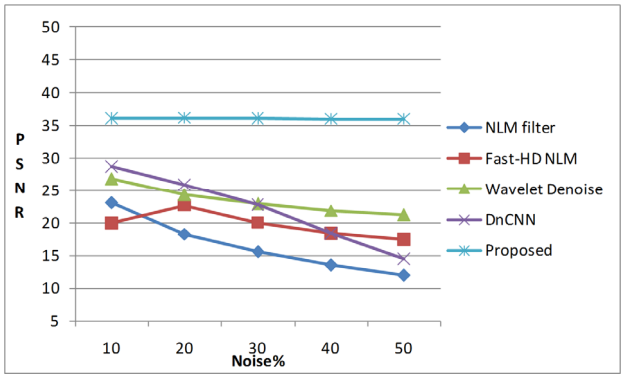

Graph 1: PSNR Consistency Graph

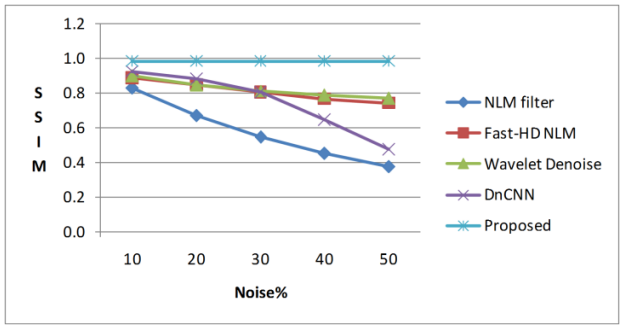

Graph 2: SSIM consistency Graph.

Figure 7: Performance of Hibiscus image for 10% AWGN.

Figure 8: Performance of Hibiscus image for 30% AWGN

Figure 9 Performance of Hibiscus image for 50% AWGN

Table 4 : Consistency of the PSNR v/s noise level.

Lenacolor.jpg					
Filter\Noise STD%	**10**	**20**	**30**	**40**	**50**
NLM Filter	23.1053	18.3260	15.5274	13.5075	11.9682
Fast HD-NLM	19.9951	22.7233	20.0303	18.3720	17.4061
Wavelet Denoise	26.8414	24.3335	22.9135	21.9318	21.2020
DnCNN	28.6880	25.9204	22.8300	18.4380	14.4755
Proposed	**36.0927**	**36.1752**	**36.0693**	**36.0307**	**35.9993**
Peppers.bmp					
Filter\Noise STD%	**10**	**20**	**30**	**40**	**50**
NLM Filter	23.7331	18.7847	15.9669	13.5110	12.1536
Fast HD-NLM	26.2509	22.3108	19.7218	18.4416	17.4061
Wavelet Denoise	28.2445	25.6329	24.1495	23.2024	22.3674
DnCNN	30.3730	27.4445	23.7130	18.7040	14.6234
Proposed	**37.3303**	**37.4168**	**37.3958**	**37.3570**	**37.3525**
Hibiscus.bmp					
Filter\Noise STD%	**10**	**20**	**30**	**40**	**50**
NLM Filter	23.6278	19.0647	16.1507	14.1225	12.3002
Fast HD-NLM	26.7977	23.7610	21.5645	20.3864	19.7685
Wavelet Denoise	29.6195	26.8788	25.2699	24.2664	23.5429
DnCNN	31.3920	28.2648	24.4410	19.0270	14.7213
Proposed	**51.1430**	**51.1505**	**51.0557**	**51.0445**	**51.0636**
Tulips.png					
Filter\Noise STD%	**10**	**20**	**30**	**40**	**50**
NLM Filter	22.4045	17.8361	15.2487	13.2508	13.2361
Fast HD-NLM	26.7945	21.8833	18.7004	17.1780	16.3904
Wavelet Denoise	28.0485	24.9647	23.3650	22.2036	21.4313
DnCNN	30.1520	26.8221	23.3900	18.6860	14.6098
Proposed	**45.3433**	**45.4116**	**45.3834**	**45.2924**	**45.2986**

Table 5 SSIM consistency v/s noise level.

Lenacolor.jpg					
Filter\Noise STD%	**10**	**20**	**30**	**40**	**50**
NLM Filter	0.8294	0.6698	0.5469	0.4508	0.3775
Fast HD-NLM	0.8892	0.8489	0.8034	0.7666	0.7422
Wavelet Denoise	0.8985	0.8479	0.8129	0.7865	0.7695
DnCNN	0.9258	0.8822	0.8049	0.6465	0.4739
Proposed	**0.9840**	**0.9843**	**0.9840**	**0.9839**	**0.9838**
Peppers.bmp					
Filter\Noise STD%	**10**	**20**	**30**	**40**	**50**
NLM Filter	0.9053	0.7787	0.6662	0.4502	0.4798
Fast HD-NLM	0.9592	0.9143	0.8726	0.8477	0.7422
Wavelet Denoise	0.9655	0.9422	0.9227	0.9085	0.8948
DnCNN	0.9771	0.9584	0.9070	0.7691	0.5897
Proposed	**0.9951**	**0.9952**	**0.9952**	**0.9952**	**0.9952**
Hibiscus.bmp					
Filter\Noise STD%	**10**	**20**	**30**	**40**	**50**
NLM Filter	0.8856	0.7778	0.6887	0.6221	0.5609
Fast HD-NLM	0.9592	0.9300	0.8991	0.8794	0.8681
Wavelet Denoise	0.9739	0.9528	0.9311	0.9185	0.9044
DnCNN	0.9799	0.9603	0.9035	0.7715	0.6346
Proposed	**0.9997**	**0.9997**	**0.9997**	**0.9997**	**0.9997**
Tulips.png					
Filter\Noise STD%	**10**	**20**	**30**	**40**	**50**
NLM Filter	0.7248	0.5462	0.4356	0.3528	0.3533
Fast HD-NLM	0.9005	0.8192	0.7182	0.6510	0.6121
Wavelet Denoise	0.8927	0.8247	0.7861	0.7458	0.7252
DnCNN	0.9312	0.8767	0.7604	0.5643	0.4014
Proposed	**0.9968**	**0.9968**	**0.9968**	**0.9968**	**0.9968**

Despite being a hybrid of Fast HD-NLM and wavelet denoising techniques, the outcome of this approach is significantly improved. Graph 3 and Graph 4 show how it works.

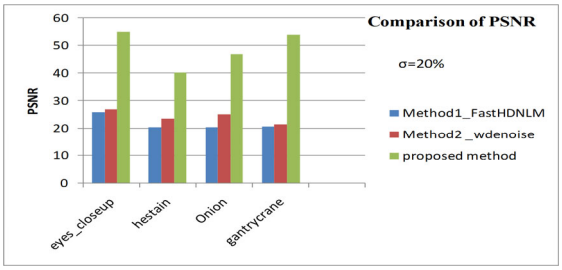

Graph 3: Improvement of PSNR against base techniques

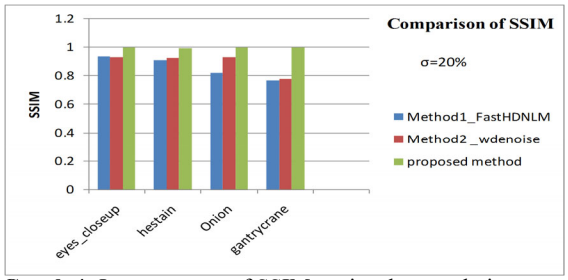

Graph 4: Improvement of SSIM against base techniques

The computing brilliance of the suggested solutions is further proven in Table VI for hestain, onion, and, gantrycrane images. In terms of NMSE and computation time, the proposed strategy beats the existing techniques such as BILF[14], MSMF[27], FDNLM[25], GNLMKIM[28], and INLM[10]. The output image clarity of fig.10, 11, and 12 demonstrates the algorithm's robustness and effectiveness.

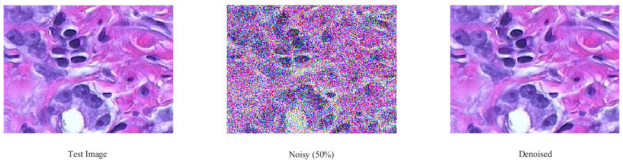

Figure 10: Image quality of denoised hestain image for 50% noise.

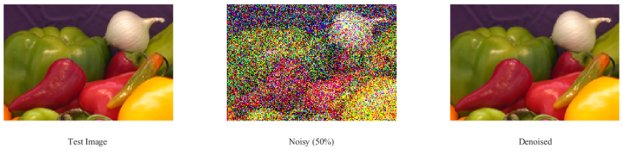

Figure 11: Image quality of denoised Onion image for 50% noise.

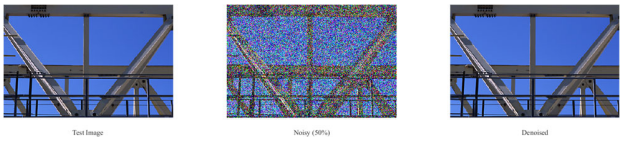

Figure 12 : Image quality of denoised Gantrycrane image for 50% noise.

5. Conclusion and Future Scope

An efficient and lightweight algorithm is proposed for removing noise from multispectral images. The empirical findings show the algorithm's uniqueness, especially its resilience, consistency as well as its noise independent performance. The success of the approach is discovered to be dependent on the remodeling of the current PCA-based NLM and its method noise shrinkage. The proposed model exhibits competitive performance outcomes with the state-of-the-art technologies of color image denoising.

This research paves the way for a fascinating investigation of the basic changes in the design of the current NL-Means models or wavelet thresholding techniques. Another worthwhile investigation is the design of a single model that can enhance performance without sacrificing visual quality. Future research suggests investigating the chance of applying the proposed model to applications like image segmentation and edge identification.

6. References

[1] J. Russ and F. Neal, "Correcting Imaging Defects," *The Image Processing Handbook, Seventh Edition*, vol. 0, pp. 163–242, 2015, doi: 10.1201/b18983-5.

[2] L. Fan, F. Zhang, H. Fan, and C. Zhang, "Brief review of image denoising techniques," *Visual Computing for Industry, Biomedicine, and Art*, vol. 2, no. 1, 2019, doi: 10.1186/s42492-019-0016-7.

[3] A. Buades, B. Coll, and J. M. Morel, "A review of image denoising algorithms, with a new one," *Multiscale Modeling and Simulation*, vol. 4, no. 2. Society for Industrial and Applied Mathematics, pp. 490–530, Jul. 26, 2005, doi: 10.1137/040616024.

[4] B. Coll, A. Buades, and J.-M. Morel, "Image and movie denoising by nonlocal means PSF Estimation View project Earth Observation and Stereo Vision View project Image and movie denoising by nonlocal means." [Online]. Available: https://www.researchgate.net/publication/240712613.

[5] R. R. Kishore and Sunesh, "Experimental analysis of color image scrambling in the spatial domain and transform domain," *International Journal of Advanced Computer Science and Applications*, vol. 10, no. 6, pp. 325–333, 2019, doi: 10.14569/ijacsa.2019.0100642.

[6] S. O. Shim, "Noise reduction on bracketed images for high dynamic range imaging," *International Journal of Advanced Computer Science and Applications*, vol. 11, no. 8, pp. 150–157, 2020, doi: 10.14569/IJACSA.2020.0110820.

[7] D. A. Kumari and A. Govardhan, "Noise reduction in spatial data using machine learning methods for road condition data," *International Journal of Advanced Computer Science and Applications*, vol. 11, no. 1, pp. 154–163, 2020, doi: 10.14569/ijacsa.2020.0110120.

[8] P. Nair and K. N. Chaudhury, "Fast High-Dimensional Bilateral and Nonlocal Means Filtering," Nov. 2018, doi: 10.1109/TIP.2018.2878955.

[9] C. Tomasi and R. Manduchi, "Bilateral filtering for gray and color images," in *IEEE International Conference on Computer Vision*, 1998, pp. 839–846.

[10] M. Zhang and B. K. Gunturk, "Multiresolution bilateral filtering for image denoising," *IEEE Transactions on Image Processing*, vol. 17, no. 12, pp. 2324–2333, 2008, doi: 10.1109/TIP.2008.2006658.

[11] A. V. Le, S. W. Jung, and C. S. Won, "Directional joint bilateral filter for depth images," *Sensors (Switzerland)*, vol. 14, no. 7, pp. 11362–11378, 2014, doi: 10.3390/s140711362.

[12] A. Buades, B. Coll, and J.-M. Morel, "Non-Local Means Denoising," *Image Processing On Line*, vol. 1, pp. 208–212, 2011, doi: 10.5201/ipol.2011.bcm_nlm.

[13] G. Wang, Y. Liu, W. Xiong, and Y. Li, "An improved non-local means filter for color image denoising," *Optik*, vol. 173, pp. 157–173, Nov. 2018, doi: 10.1016/j.ijleo.2018.08.013.

[14] P. A. Shyjila and M. Wilscy, "Non local means image denoising for color images using PCA," *Communications in Computer and Information Science*, vol. 131 CCIS, no. PART 1, pp. 288–297, 2011, doi: 10.1007/978-3-642-17857-3_29.

[15] D. DONOHO and I. JOHNSTONE, "Ideal denoising in an orthonormal basis chosen from a library of bases," *Comptes rendus de l'Académie des sciences. Série I, Mathématique*, vol. 319, no. 12, pp. 1317–1322, 1994.

[16] *Advances in Wavelet Theory and Their Applications in Engineering, Physics and Technology*. 2012.

[17] P. Hedaoo and S. S. Godbole, "Wavelet Thresholding Approach For Image Denoising," *International Journal of Network Security & Its Applications*, vol. 3, no. 4, pp. 16–21, 2011, doi: 10.5121/ijnsa.2011.3402.

[18] R. Guhathakurta, "Denoising of image: A wavelet based approach," *2017 8th Industrial Automation and Electromechanical Engineering Conference, IEMECON 2017*, pp. 194–197, 2017, doi: 10.1109/IEMECON.2017.8079587.

[19] D. Cho, T. D. Bui, and G. Chen, "Image denoising based on wavelet shrinkage using neighbor and level dependency," *International Journal of Wavelets, Multiresolution and Information Processing*, vol. 7, no. 3, pp. 299–311, 2009, doi: 10.1142/S0219691309002945.

[20] F. Xiao and Y. Zhang, "A comparative study on thresholding methods in wavelet-based image denoising," *Procedia Engineering*, vol. 15, pp. 3998–4003, 2011, doi: 10.1016/j.proeng.2011.08.749.

[21] S. Ruikar and D. D. Doye, "Image denoising using wavelet transform," *ICMET 2010 - 2010 International Conference on Mechanical and Electrical Technology, Proceedings*, no. February, pp. 509–515, 2010, doi: 10.1109/ICMET.2010.5598411.

[22] X. P. Zhang and M. D. Desai, "Adaptive denoising based on SURE risk," *IEEE Signal Processing Letters*, vol. 5, no. 10, pp. 265–267, 1998, doi: 10.1109/97.720560.

[23] L. Zhang, W. Dong, D. Zhang, and G. Shi, "Two-stage image denoising by principal component analysis with local pixel grouping," *Pattern Recognition*, vol. 43, no. 4, pp. 1531–1549, 2010, doi: 10.1016/j.patcog.2009.09.023.

[24] A. A. Ismael and M. Baykara, "Digital image denoising techniques based on multi-resolution wavelet domain with spatial filters: A review," *Traitement du Signal*, vol. 38, no. 3, pp. 639–651, 2021, doi: 10.18280/ts.380311.

[25] B. K. Shreyamsha Kumar, "Image denoising based on gaussian/bilateral filter and its method noise thresholding," *Signal, Image and Video Processing*, vol. 7, no. 6, pp. 1159–1172, 2013, doi: 10.1007/s11760-012-0372-7.

[26] P. Nair and K. N. Chaudhury, "Fast high-dimensional bilateral and nonlocal means filtering," *IEEE Transactions on Image Processing*, vol. 28, no. 3, pp. 1470–1481, 2019, doi: 10.1109/TIP.2018.2878955.

[27] K. Zhang, W. Zuo, Y. Chen, D. Meng, and L. Zhang, "Beyond a Gaussian denoiser: Residual learning of deep CNN for image denoising," *IEEE Transactions on Image Processing*, vol. 26, no. 7, pp. 3142–3155, Jul. 2017, doi: 10.1109/TIP.2017.2662206.

[28] T. Tasdizen, "Principal neighborhood dictionaries for nonlocal means image denoising," *IEEE Transactions on Image Processing*, vol. 18, no. 12, pp. 2649–2660, 2009, doi: 10.1109/TIP.2009.2028259.

Author Details

Vijayalaxmi Hegde has a master's degree in electronics from Karnatak University Dharwad and a master's degree in information technology from Mysore.
She currently works as an assistant professor at M.E.S.M.M. Arts and Science College Sirsi in Uttara Kannada. She is also a research scholar at Kuvempu University's Department of Postgraduate Studies and Research in Electronics in Shimoga, India. Digital Image Processing, Wireless Sensor Networks, and Embedded Systems are among the research interests of this group.

Dr. Basavaraj N Jagadale is an Associate Professor at Kuvempu University in Shimoga, India, in the Department of Postgraduate Studies and Research in Electronics. He holds a PhD from Karnataka University in Dharwad, India. During 2015-16, he worked in the Radiology Department at the University of Pennsylvania, USA, as part of a UGC Raman fellowship given by the Indian government for post-doctoral research. His research interests are in signal and image processing, and he has published more than 30 publications in peer-reviewed journals. He has also served as a journal reviewer.

Mukund N Naragund has an MSc (Electronics) from Karnataka University in Dharwad, India, an MPhil from Bharathidasan University in Trichy, India, and a Ph.D from Kuvempu University in Shankaraghatta. He is an Associate Professor at the Physics and Electronics Department of CHRIST (Deemed to be University) in Bengaluru, India. Digital logic design, Verilog, FPGA, Embedded systems, and Electronic Instrumentation are among his teaching specialties. His field of study is digital image processing.